5G Stochastic Channel Modelling

A Project Report

Submitted by

K Sai Vasu Deeraj
(EE16B018)

in the partial fulfilment of the requirements
for the award of the degree of

BACHELOR OF TECHNOLOGY
in
ELECTRICAL ENGINEERING

DEPARTMENT OF ELECTRICAL ENGINEERING

INDIAN INSTITUTE OF TECHNOLOGY MADRAS

CHENNAI-600036

JUNE 2020

THESIS CERTIFICATE

This is to certify that the thesis entitled **"5G Stochastic Channel Modelling"** submitted by "**K Sai Vasu Deeraj"** to the Indian Institute of Technology, Madras for the award of the degree of BACHELOR OF TECHNOLOGY in ELECTRICAL ENGINEERING is a bona fide record of research work carried out by him under my supervision. The contents of this thesis, in full or in parts, have not been submitted to any other Institute or University for the award of any degree or diploma.

Prof. Radha Krishna Ganti
Associate Professor
Department of Electrical Engineering
Indian Institute of Technology Madras
Chennai – 600 036.

TABLE OF CONTENTS

Contents

TABLE OF CONTENTS 3

LIST OF FIGURES 4

CHAPTER 1 5

Introduction 5

1.1 Factors for advancing to 5G 5

1.2 The 5G Testbed in India 6

My Contribution in this project 6

CHAPTER 2 7

2.1 Project Statement 7

2.2 Literature review 7

2.2.1 Introduction to IMT-2020 7

2.2.2 Evaluation procedures 7

2.2.3 Minimum Key Requirements 8

2.2.4 Usage Scenarios 8

Test environments in IMT-2020 primary module 8

CHAPTER 3 10

3.1 Channel Model Approach - 5G Stochastic Channel Modelling 10

3.2 Step-by-step procedure 14

3.3 Field pattern generation: 26

CHAPTER 4 28

4.1 ANTENNA RADIATION PATTERN (contributed by my project mate M.S. Ajay) 28

4.2 CHANNEL ESTIMATION (contributed by me) 30

4.3 SINR GENERATION (contributed by M.S. AJAY) 32

CHAPTER 5 35

Potential extensions and future work 35

Summary 35

References: 36

LIST OF FIGURES

All the following figures are generated using the MATLAB code.

Figure – 4.1 : This shows how the antenna element radiation pattern varies from elevational angle perspective.

Figure – 4.2 : This shows how the antenna element radiation pattern varies from azimuthal angle perspective.

Figure – 4.3 : This shows how the antenna element radiation pattern varies in 3-D plot.

Figure – 4.4 : This shows how the antenna array radiation pattern varies from elevational angle perspective.

Figure – 4.5 : This shows how the antenna array radiation pattern varies from azimuthal angle perspective.

Figure – 4.6 : This shows how the antenna array radiation pattern varies in 3-D plot.

Figure – 4.7 : This shows the Channel gains for all the 3072 sub-carriers for RMa_A profile.

Figure – 4.8 : This shows the Channel gains for all the 3072 sub-carriers for UMa_A profile.

Figure – 4.9 : This shows the Channel gains for all the 3072 sub-carriers for UMi_A profile.

Figure – 4.10 : This shows the Channel gains for all the 3072 sub-carriers for InH_A profile.

Figure – 4.11 : The figure captures the SINR for RURAL profile and LOS condition.

Figure – 4.12 : The figure captures the SINR for RURAL profile and NLOS condition.

Figure – 4.13 : The figure captures the SINR for URBAN profile and LOS condition.

Figure – 4.14 : The figure captures the SINR for URBAN profile and NLOS condition.

CHAPTER 1

Introduction

1.1 Factors for advancing to 5G

Through the evolution of cellular standards, new countries have joined the making process of these cellular standards and India has also become a small part in bringing up the 5G ecosystem along with countries like South Korea, USA, China and Europe.

Today cellular technology has become a common man's technology and the market for it has grown manifolds. While 4G managed to provide good enough data rates, they were not designed to support extremely high data rates, low latency to support real time applications like automated vehicles or to support a large number of IOT devices, which clearly are the order of the day. These are the key motivating factors to bring in 5G, designed to support speed of 10 Gbps.

The key factor enabling drastic differences in data speeds in 5G, is the use of mm Wave spectrum bands, frequencies above 20GHz. Though there is a flipside of the issue of transmitting signals efficiently at these frequencies, which have been tackled with the help of technologies like phased arrays, they provide much larger bandwidths compared to the lower frequencies used in earlier standards like 700 MHz or 4GHz, thus increasing the data capacity manifolds.

The International Telecom Union (ITU) is the body that defines each generation of these cellular/ wireless standards and makes sure the spectrum needed for these standards are allocated accordingly. It is an UN agency that legally binds all of its member countries. 3G/CDMA was defined by IMT-2000, 4G/LTE by IMT-Advanced and 5G by IMT-2020. The ITU essentially defines the targets of KPIs like user experienced data rate, peak and average spectral efficiency, to list a few examples, that are to be met by each cellular standard/ generation developed.

The Third Generation Partnership Project (3GPP) initially set up to bring about the 3G standard, is the body that makes the cellular technology to meet the ITU and consumer requirements. It is made up of key technology companies and research labs and has been the significant contributor in developing 3G, 4G and 5G standards and all the existing standards are complaint with those made by 3GPP. It submits the proposed technology to ITU for ratification. The ITU has independent bodies which verify if they meet the set standards.

1.2 The 5G Testbed in India

The IITM 5G testbed, as a part of the 5G testbed comprising a lot of institutes and industrial contributors with funding from the Department of Telecommunications (DOT), has been developing the 5G standard specifically for Indian markets. The major goal has been to bring up the deployment of 5G standard in India and to increase India's participation in global forums like 3GPP and ITU and present the test/ evaluation results for Indian use cases.

The part of the project involved developing the 5G Stochastic Channel Model (SCM) proposed by 3GPP, done in MATLAB as a part of the own simulator being built in the IITM 5G testbed for carrying out the evaluation procedures. This simulator provides more flexibility in the simulation procedures as we have full control over setting the configuration parameters

The channel model is built as defined in the ITU document M.2412 defining the evaluation procedures. The document explains in detail about the small scale and large-scale parameters generation procedure for each test environment and usage scenarios, explained in detail in the later part of this report, which are then used to generate the channel coefficients between transmit and receive antennas.

My Contribution in this project

The initial version of the 5G SCM channel model created in MATLAB for simulations is for the case of a single transmission link between single antenna elements at the transmitter and receiver. The extension of the same to the case when multiple antenna panels are used was later done. The final channel coefficient results are a 2-D array and a 4-D array respectively for the cases mentioned.

My work specifically involved in creating the functions required for executing **Steps 2 (Prob_LOS), 3(only pathloss excluding indoor loss and in car loss), 5 to 7(delay, power and generation of angles), and Steps 9 – 11**. My work for **step-11** included coefficient generation for **element to element**, later it was developed into antenna array by my fellow project mate Preethi. I also worked for the **code generating the plots of channel estimation**.

My project mate Preethi contributed step-4, 7 and step-11 in upgrading it to the antenna array. She hardcoded all the values from the document to code to generate LSP in step-4. All the means, variances and correlation matrices.

My project mate M.S. Ajay contributed step-3 (indoor loss and in car loss), step-8 (coupling) and interpolation of H coefficients using SINC function, calculating field pattern, plotting antenna radiation power pattern and finally SINR distribution.

This report includes the total work by the team, I mentioned the work done by be wherever necessary.

CHAPTER 2

2.1 Project Statement

Create the 5G SCM channel model in MATLAB to create channel coefficients between individual channels for a set of multiple gNBs and UEs per sector. These coefficients are to be used for getting a received signal when a 5G signal is transmitted and subsequently use it to measure the SINR and other KPIs required for self-evaluation. This channel model will be used as a part of the own simulator created in the IITM 5G testbed.

2.2 Literature review

2.2.1 Introduction to IMT-2020

International Mobile Telecommunications-2020 (IMT-2020) systems are mobile systems that include new radio interface(s) which support the new capabilities of systems beyond IMT-2000 and IMT-Advanced. The ITU-R M.2083 recommendation explains the capabilities of IMT-2020.

The recommendation aims to make IMT-2020 more flexible, reliable and secure than previous IMT when services are provided in the intended three usage scenarios, namely enhanced mobile broadband (eMBB), ultra-reliable and low-latency communications (URLLC), and massive machine type communications (mMTC).

2.2.2 Evaluation procedures

The evaluation procedures, following the evaluation configurations for simulations, are done as explained in the ITU document M.2412 across a number of test environments, which are chosen to simulate environments that are as close as possible to the more real stringent radio operating environments.

Evaluation of proposals can be done through simulation, analytical and inspection procedures. Each proposal is evaluated to verify if the key minimum technical performance requirements are met as defined in the ITU-R M.2410 document.

The self-evaluation report is then done following the guidelines in ITU-R M.2412 and submitted for assessment of the proposed RITs/SRITs.

2.2.3 Minimum Key Requirements

The key minimum technical performance requirements are defined for the purpose of consistent definition and evaluation of the candidate IMT-2020 RITs/SRITs.

There are 13 of them listed in the ITU-R M.2410 document. They are as listed below:

1. Peak data rate
2. Peak spectral efficiency
3. User experienced data rate
4. 5th percentile user spectral efficiency
5. Average spectral efficiency
6. Area traffic capacity
7. Latency
8. Connection density
9. Energy efficiency
10. Reliability
11. Mobility
12. Mobility interruption time
13. Bandwidth

The high-level assessment method (simulation/ analytical/ inspection) to be used for evaluating each one of the above KPIs along with the corresponding evaluation procedure is given in ITU-R M.2412 and the same is followed while carrying out the self-evaluation procedure.

2.2.4 Usage Scenarios

The proposed RIT/SRIT shall support a wide range of services across different usage scenarios like:

- ***eMBB*** - Enhanced Mobile Broadband
- ***mMTC*** - Massive machine type communications
- ***URLLC*** - Ultra-reliable and low latency communications

Test environments in IMT-2020 primary module

IMT-2020 covers the usage scenarios eMBB, URLLC and mMTC across the Indoor Hotspot, Urban and Rural test environments. IMT primary module defines Channel A and B for each of the test environment based on field measurements and are both valid for IMT-2020 candidate evaluations. The mapping of the channel models with the test environments is as shown below.

Test environment	**Indoor Hotspot-eMBB**	**Rural- eMBB**	**Dense Urban -eMBB**	**Urban Macro-URLLC**	**Urban Macro-mMTC**
Channel model	InH_A, InH_B	RMa_A, RMa_B	**Macro layer:** UMa_A, UMa_B **Micro layer:** UMi_A, UMi_B	UMa_A, UMa_B	UMa_A, UMa_B

Evaluation configurations are defined for the selected test environments. The configuration parameters are applied in analytical and simulation assessments of candidate RITs/SRITs. The technical performance requirement corresponding to that test environment is fulfilled if this requirement is met for one of the evaluation configurations under that specific test environment.

CHAPTER 3

3.1 Channel Model Approach - 5G Stochastic Channel Modelling

Channel modelling is required for realistically modelling the propagation conditions for radio transmission for all required test environments and usage scenarios. There are three IMT-2020 channel modules described in ITU-R M.2412 namely, the primary, extension and map-based hybrid modules. The project involved modelling the channel based on Primary module, which is a geometry-based stochastic channel model.

A Single Input Single Output (SISO) channel is characterized by two domains, time and frequency and the multipath propagation is defined by attenuation, time delay and path phase.

The Multiple Input Multiple Output (MIMO) channel however is characterized by four domains: Time, Frequency, Space, Polarization. The channel coefficients depend on the transmit and receive antenna characteristics and the propagation characteristics.

The MIMO channel models can either be physical or analytical. Physical models are based on physical theory (often geometrical optics) or on physical measurements. Analytical models are based on mathematical assumptions about the channel behaviour. A physical model further can be either deterministic, where the output of the model is fully determined by the parameter values or stochastic models which possess inherent randomness and the same set of parameter values can lead to an ensemble of output values.

In the Primary Module used for designing the channel model, instead of specifying the location of the scatterers explicitly, the direction of rays is used. This geometry-based modelling enables separation of propagation parameters and antennas.

In the absence of environmental scatterers, we get a single pure LOS path (Fig-3.1).

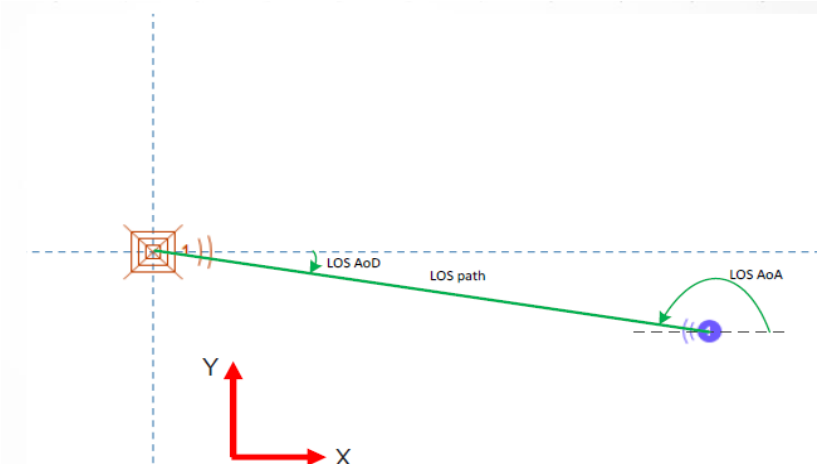

Figure – 3.1

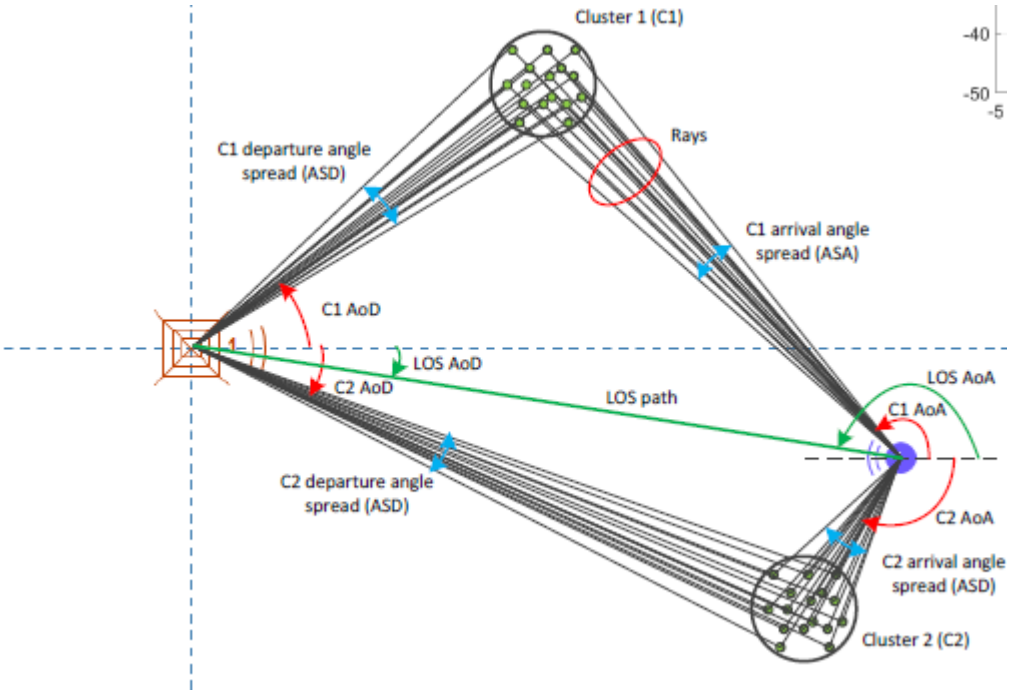

Figure – 3.2

But in the presence of environmental scatterers, multiple propagation paths or (rays) are scattered from buildings etc rather than a LOS path. Scattering from such rough surfaces results as groups of rays close to each dominant propagation path, resulting in the concept of Clusters, as depicted in Fig – 3.2.

Clusters are defined by angular characteristics like Angular Spread of Departure (ASD), Angular Spread of Arrival (ASA), Angle of Departure (AOD) and Angle of Arrival (AOA) in stochastic models.

The channel parameters are determined stochastically based on statistical distributions from channel measurements. The channel is then realized through the application of the geometrical principle by summing the contributions of rays with specific small-scale parameters like delay, power, azimuth angles of arrival and departure and elevation angles of arrival and departure, which results in correlation of antenna elements and fading due to Doppler as well.

In the absence of a detailed environment database, the precise physical propagation parameters like Direction of Departure (DOD), Direction of Arrival (DOA), number of paths, path delay, path power are unpredictable, but they have well defined statistical behaviours. Probability models can therefore be constructed for these propagation parameters.

The 3D MIMO channel model

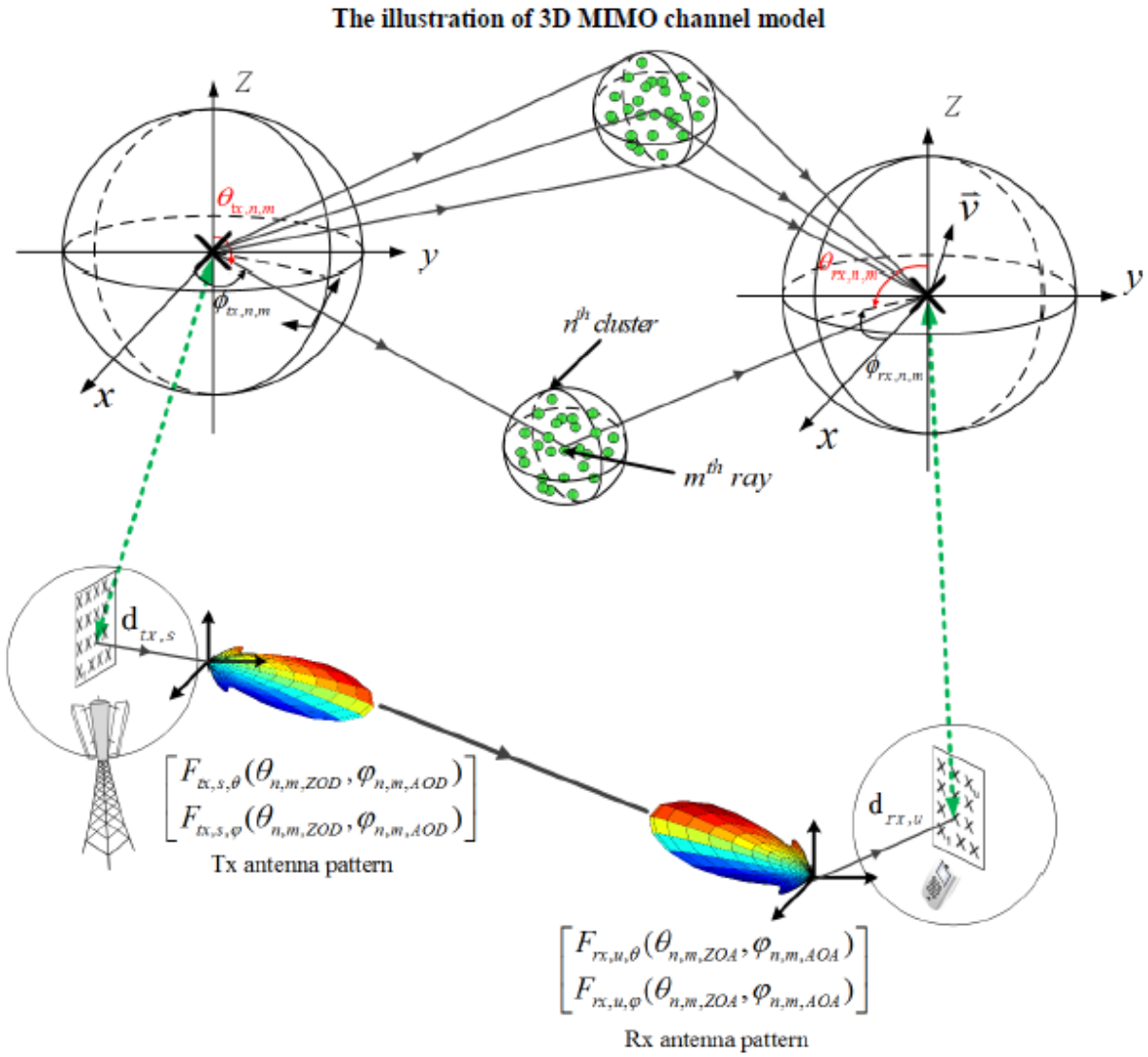

Figure 3.3

The above illustration is for a single link channel model. Each circle with several dots represents a scattering region causing one cluster. Each cluster is constituted by *M* rays, and we assume N clusters and *S* antenna elements for transmitter (Tx) and *U* antenna elements for receiver (Rx), respectively. The small-scale parameters like delay $\tau_{n,m}$, azimuth angle of arrival $\varphi_{rx,n,m}$, elevation angle of arrival $\theta_{rx,n,m}$, azimuth angle of departure $\varphi_{tx,n,m}$ and elevation angle of departure $\theta_{tx,n,m}$ are assumed to be different for each ray, where *n*, *m, u, s* are the indices of the cluster, ray, receiver element and transmitter element

respectively. $d_{rx,u}$ and $d_{tx,s}$ are the location vectors of the receive antenna element *u* and transmit antenna element s.

Procedure to generate the channel coefficients

The channel is realised through a detailed step-step procedure consisting of 12 steps as shown below. Apart from this, the advanced channel modelling options described in ITU-R M.2412 can be used for simulating certain cases during the evaluation procedure as well.

The geometric description is such that the arrival angle is from the last scattered bounce and the departure angle is to the first scattered from the transmitting side. Thus, the propagation between the first and last interaction is not defined and this allows for modelling multiple interactions in the scattering media. Therefore, parameters like delay can't be deduced from geometry and the procedure for generating such parameters is described in the document.

The following steps are defined for the downlink scenario. For the uplink scenario, the departure and arrival parameters are swapped.

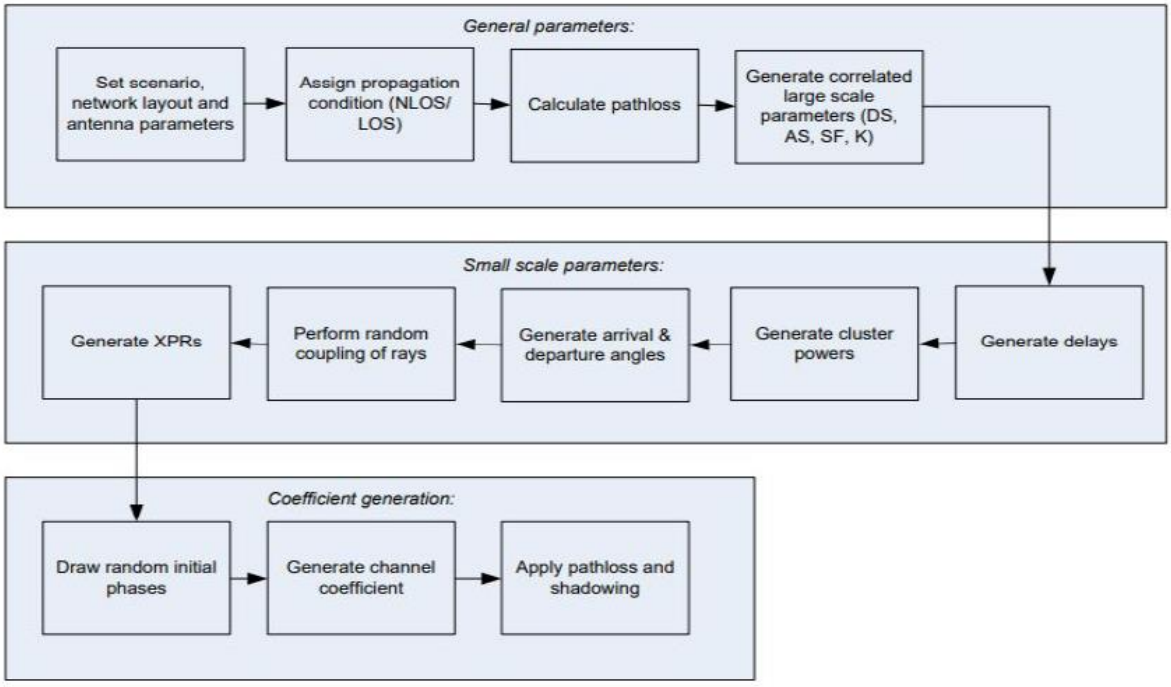

Figure 3.4 – Flow chart of generating Channel coefficients

Coordinate System

The coordinate system to be followed is defined by the x, y, z axes, spherical angles and vectors as shown in the figure below. The zenith angle(θ) and azimuth angle(φ) are defined

in the Cartesian system as shown below. The spherical basis vectors $\hat{\theta}$ and $\hat{\varphi}$ are defined based on the propagation direction $\hat{n}$. The field component in the direction of $\hat{\theta}$ is given by F_θ and the field component in the direction of $\hat{\varphi}$ is given by F_φ.

Definition of a global coordinate system showing the zenith angle θ and the azimuth angle ϕ

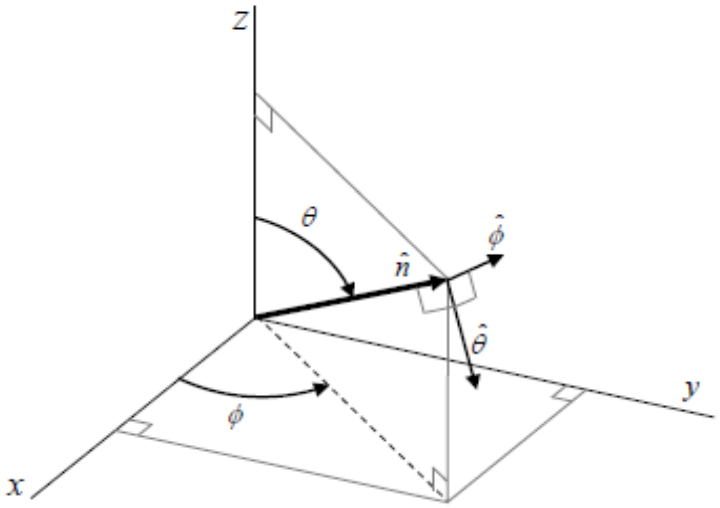

Figure 3.5 - GCS

3.2 Step-by-step procedure

Step 1: Setting environment, network layout, and antenna array parameters

- Choose one of the test environments and corresponding network layouts
- Choose a global coordinate system and define the zenith and azimuth angles and spherical unit vectors as discussed earlier.
- Give the number of Base Station (BS) and User Terminals (UT).
- Give 3D location of BS and UT and determine LOS AOD, LOS ZOD, LOS AOA, LOS ZOA.
- Give BS and UT antenna field patterns F_{rx} and F_{tx} in the global coordinate system and array geometries.
- Give BS and UT array orientations with respect to the global coordinate system
- Array orientation is defined by three angles: Bearing angle, down tilt angle, slant angle
- Give speed and direction of motion of UT in the global coordinate system.
- Give system centre frequency *fc* and bandwidth B.

Step 2: Propagation condition LOS/NLOS

- Assign propagation condition (LOS/NLOS).
- The propagation conditions for different BS-UT links are uncorrelated.
- LOS is a probability distribution which depends on distance from BS and height of

UT. This distribution is different for indoor and outdoor state.

- Assign an indoor/outdoor state for each UT.
- All the links from a single UT have the same indoor/outdoor state.

Step 3: Modelling and calculation of pathloss

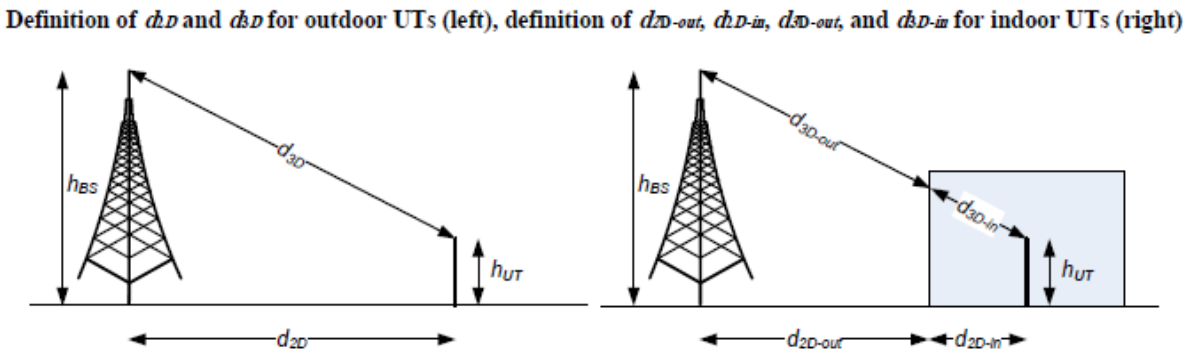

Figure 3.6

- h_{UT} and h_{BS} are the antenna height at BS and UT, respectively.
- Pathloss depends on LOS/NLOS condition, the distance between BS and UT and frequency of carrier f_c.
- Different pathloss models have been specified for different test environments in the ITU document for 2 frequency ranges: one in the range 0.5 GHz - 6 GHz and the other, those above 6 GHz. (Refer ITU-R M.2412-0)
- In addition to this, outdoor to indoor (O-I) building penetration and car penetration losses should also be taken into account.

Step 4: Generation of LSPs

Large scale parameters listed below are generated in this step:

- Root-mean-square delay spread (DS)

  The maximum delay time spread is the total time interval during which reflections with significant energy arrive. The R.M.S. delay spread is the standard deviation (or root-mean-square) value of the delay of reflections, weighted proportional to the energy in the reflected waves.

- Root-mean-square angular spreads: Azimuth Angle Spread of Arrival (ASA), Azimuth Angle Spread of Departure (ASD), Zenith Angle Spread of Arrival (ZSA) and Zenith Angle Spread of Departure (ZSD)

- Ricean K-factor (K)

The ratio of signal power in dominant component over the (local-mean) scattered power.

- Shadow fading (SF)

All these LSPs are correlated and the correlated LSPs are generated taking into account the cross-correlation parameters given in the ITU document using the procedure described in § 3.3.1 of WINNER II Channel Models [4].

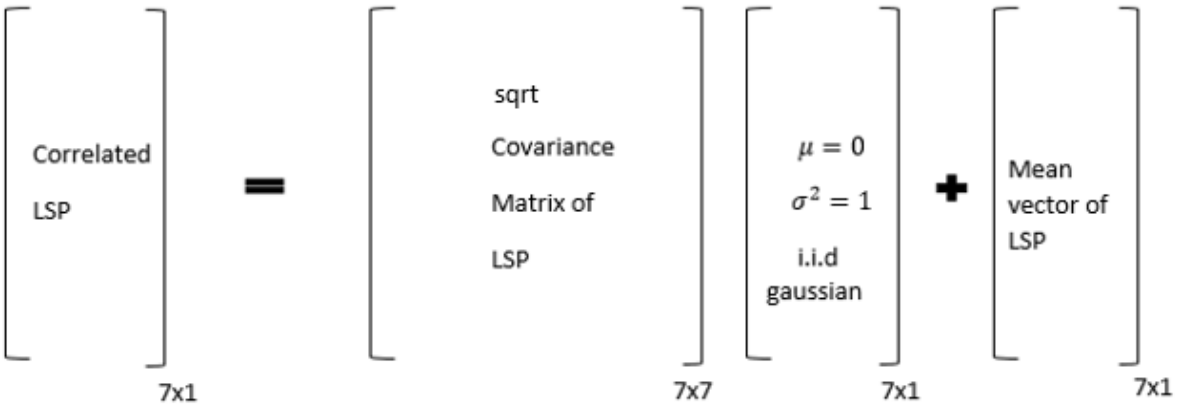

Generation of Small-scale parameters

Step 5: Generation of delays

Delays are drawn randomly from an exponential delay distribution and are calculated as:

$$\tau_n' = - r_\tau \, DS \, ln \, (X_n)$$

where r_τ is the delay distribution proportionality factor, X_n ~ uniform (0,1), and n is the cluster index n = 1, . . ., N.

The delays are then normalised by subtracting the minimum delay and are then sorted in the ascending order.

$$\tau_n = sort \, (\tau_n' - min \, (\tau_n'))$$

In the case of LOS condition, additional scaling of delays is required to compensate for the effect of LOS peak addition to the delay spread. The Ricean K-factor dependent scaling constant is:

$$C_K = 0.7705 - 0.0433 \, K + 0.002 \, K^2 + 0.000017 \, K^3$$

where K [dB] is the Ricean K-factor as generated in Step 4.

The scaled delays $\tau_n^{LOS} = \tau_n / C_K$ are not to be used in cluster power generation.

Step 6: Generation of cluster powers

Cluster powers are calculated, assuming a single slope exponential power delay profile. Power assignment depends on the exponential delay distribution. The cluster powers are determined by:

$$P_n' = exp\left(-\tau_n \frac{r_\tau - 1}{r_\tau \mathrm{DS}}\right) \cdot 10^{\frac{-Z_n}{10}}$$

where $Z_n \sim N(0, \zeta^2)$ is the per cluster shadowing term in [dB]
The cluster powers are then normalised so that the sum power of all cluster powers is equal to one.

$$P_n = \frac{P_n'}{\sum_{n=1}^{N} P_n'}$$

In the case of LOS condition, an additional specular component is added to the first cluster. The power of the single LOS ray is given by:

$$P_{1,LOS} = \frac{K_R}{K_R + 1}$$

And the cluster powers are given by:

$$P_n = \frac{1}{K_R + 1} \frac{P_n'}{\sum_{n=1}^{N} P_n'} + \delta(n-1) P_{1,LOS}$$

The power of each ray within a cluster is assigned as *Pn/M*, where *M* is the number of rays per cluster. The clusters with less than –25 dB power compared to the maximum cluster power are then removed.

Step 7: Generation of arrival and departure angles in both dimensions

Angle generation in azimuth direction

The composite Power Azimuth Spectrum (PAS) in azimuth of all clusters can be modelled as wrapped Gaussian or Laplacian. The AOAs are determined by applying the inverse Gaussian function equation or the inverse Laplacian function equation with input parameters P_n and RMS angle spread ASA, respectively.

$$\text{Gaussian: } \varphi_{n,AOA}' = \frac{2(\text{ASA}/1.4)\sqrt{-\ln\left(P_n/\max\left(P_n\right)\right)}}{C_\varphi}$$

$$\text{Laplacian: } \phi_{n,AOA}' = -\frac{\text{ASA}\ln\left(P_n/\max\left(P_n\right)\right)}{C_\phi}$$

with C_ϕ defined as:

$$\text{Guassian: } C_\phi = \begin{cases} C_\phi^{\text{NLOS}} \cdot \left(1.1035 - 0.028K - 0.002K^2 + 0.0001K^3\right) & \text{,for LOS} \\ C_\phi^{\text{NLOS}} & \text{,for NLOS} \end{cases},$$

$$\text{Laplacian: } C_\phi = \begin{cases} C_\phi^{\text{NLOS}} \cdot \left(0.9275 + 0.0439K - 0.0071K^2 + 0.0002K^3\right) & \text{,for LOS} \\ C_\phi^{\text{NLOS}} & \text{,for NLOS} \end{cases},$$

where C_φ^{NLOS} is defined as a scaling factor related to the total number of clusters and the values for each cluster for both Laplacian and Gaussian distributions are given in the document.

A positive or negative sign is assigned to the angles by multiplying with a random variable X_n with uniform distribution to the discrete set of {1, –1}, and add a component $Y_n \sim N(0, (ASA/7)^2)$ to introduce a random variation.

$$\phi_{n,AOA} = X_n\phi'_{n,AOA} + Y_n + \phi_{LOS,AOA}$$

where $\varphi_{LOS,\,AOA}$ is the LOS direction defined in the network layout description as mentioned in Step 1.

In the LOS case, the constant C_φ also depends on the Ricean K-factor in [dB], as generated in Step 4. Additional scaling of the angles is required to compensate for the effect of LOS peak addition to the angle spread.

In the LOS case, instead of the above equation, the below equation is used so that the first cluster is forced to the LOS direction $\varphi_{LOS,\,AOA}$:

$$\phi_{n,AOA} = \left(X_n\phi'_{n,AOA} + Y_n\right) - \left(X_1\phi'_{1,AOA} + Y_1 - \phi_{LOS,AOA}\right)$$

Ray offset angles α_m for each of the rays within a cluster, are given for rms angle spread normalized to 1, in the document. These are added to the cluster angles as shown below:

$$\phi_{n,m,AOA} = \phi_{n,AOA} + c_{ASA}\alpha_m$$

where c_{ASA} is the cluster-wise rms azimuth spread of arrival angles (cluster ASA), which are also given in the document. The generation of AOD ($\varphi_{n,m,AOD}$) follows a procedure similar to AOA as described above.

Angle generation in zenith direction

The composite Power Azimuth Spectrum (PAS) in zenith of all clusters are modelled as Laplacian. The ZOAs are determined by applying the inverse Laplacian function equation with input parameters P_n and RMS angle spread ZSA, respectively.

$$\theta'_{n,ZOA} = -\frac{\mathrm{ZSA}\, ln(P_n / max(P_n))}{C_\theta}$$

For channel model A, C_θ is defined as:

$$C_\theta = \begin{cases} C_\theta^{\mathrm{NLOS}} \cdot \left(1.35 + 0.0202K - 0.0077K^2 + 0.0002K^3\right) & \text{, for LOS} \\ C_\theta^{\mathrm{NLOS}} & \text{, for NLOS} \end{cases}$$

For channel model B, C_θ is defined as:

$$C_\theta = \begin{cases} C_\theta^{\mathrm{NLOS}} \cdot \left(1.3086 + 0.0339K - 0.0077K^2 + 0.0002K^3\right) & \text{, for LOS} \\ C_\theta^{\mathrm{NLOS}} & \text{, for NLOS} \end{cases}$$

Where C_θ^{NLOS} is defined as a scaling factor related to the total number of clusters and the values for each cluster for the Laplacian distribution are given in the document.

A positive or negative sign is assigned to the angles by multiplying with a random variable X_n with uniform distribution to the discrete set of {1, –1}, and add a component Y_n ~ N (0, (ASA/7)^2) to introduce a random variation.

$$\theta_{n,ZOA} = X_n \theta'_{n,ZOA} + Y_n + \bar{\theta}_{ZOA},$$

where $\bar{\theta}_{ZOA}$ = 90° if the BS-UT link is O2I and $\bar{\theta}_{ZOA} = \theta_{LOS,\,ZOA}$ which is the LOS direction defined in the network layout description as mentioned in Step 1.

In the LOS case, instead of the above equation, the below equation is used so that the first cluster is forced to the LOS direction $\theta_{LOS,\,ZOA}$:

$$\theta_{n,ZOA} = \left(X_n \theta'_{n,ZOA} + Y_n\right) - \left(X_1 \theta'_{1,ZOA} + Y_1 - \theta_{LOS,ZOA}\right).$$

Ray offset angles α_m for each of the rays within a cluster, are given for rms angle spread normalized to 1, in the document. These are added to the cluster angles as shown below:

$$\theta_{n,m,ZOA} = \theta_{n,ZOA} + c_{ZSA}\alpha_m$$

where c_{ZSA} is the cluster-wise rms azimuth spread of arrival angles (cluster ZSA), which are also given in the document.

The generation of ZOD ($\theta_{n,m,ZOD}$) follows a similar procedure.

$$\theta_{n,ZOD} = X_n \theta'_{n,ZOD} + Y_n + \theta_{LOS,ZOD} + \mu_{offset,ZOD}$$

where X_n is a variable with uniform distribution to the discrete set of {1, –1},
Y_n ~ N (0, (ASA/7)^2) and the values for $\mu_{offset,ZOD}$ are mentioned in the document.

Ray offset angles α_m for each of the rays within a cluster, are given for rms angle spread normalized to 1, in the document. These are added to the cluster angles as shown below:

$$\theta_{n,m,ZOD} = \theta_{n,ZOD} + (3/8)(10^{\mu_{1gZSD}})\alpha_m$$

where μ_{1gZSD} is the mean of the ZSD log-normal distribution.

In the LOS case, the generation of ZOD follows the same procedure as ZOA described above using equation.

Step 8: Coupling of rays within a cluster for both dimensions

- Couple randomly AOD angles $\varphi_{n,m,AOD}$ to AOA angles $\varphi_{n,m,AOA}$ within a cluster n, or within a subcluster in the case of two strongest clusters (described in Step 11).
- Couple randomly ZOD angles $\theta_{n,m,ZOD}$ with ZOA angles $\theta_{n,m,ZOA}$ using the same procedure.
- Also, Couple randomly AOD angles $\varphi_{n,m,AOD}$ with ZOD angles $\theta_{n,m,ZOD}$ using the same procedure.

Step 9: Generation of cross polarization power ratios

The cross-polarization power ratios *K* (XPR) are generated for each ray ***m*** of each cluster ***n***. XPR is log-normal distributed. The XPR values are drawn as shown below:

$$K_{n,m} = 10^{X/10}$$

where $X \sim N(\mu_{XPR}, \sigma^2_{XPR})$ *is* Gaussian distributed with μ_{XPR}, σ^2_{XPR} values given in the document.

Generation of channel coefficients

Step 10: Drawing of initial phases

The initial phase $\{\phi_{n,m}^{\theta\theta}, \phi_{n,m}^{\theta\varphi}, \phi_{n,m}^{\varphi\theta}, \phi_{n,m}^{\varphi\varphi}\}$ is drawn randomly for each ray *m* of each cluster *n* and for four different polarisation combinations (θθ, θφ, φθ and φφ). The distribution for initial phases is uniform within (-π, +π). It is added to ensure a random starting point for fast fading.

In the LOS case, if ϕ_{LOS} is chosen as a random variable, then a random initial phase for both θθ and φφ polarisations are drawn.

Step 11: Generation of channel coefficients

Channel impulse response generation for a single link (Single antenna panel at both tx and rx)

The channel coefficients are generated for each cluster *n* and each receiver and transmitter element pair *u, s*.

For the *N – 2* weakest clusters, say n = 3, 4, *N*, the channel coefficients are given by:

$$H_{u,s,n}^{\mathrm{NLOS}}(t) = \sqrt{\frac{P_n}{M}} \sum_{m=1}^{M} \begin{bmatrix} F_{rx,u,\theta}\left(\theta_{n,m,ZOA}, \varphi_{n,m,AOA}\right) \\ F_{rx,u,\varphi}\left(\theta_{n,m,ZOA}, \varphi_{n,m,AOA}\right) \end{bmatrix}^T \begin{bmatrix} \exp\left(j\Phi_{n,m}^{\theta\theta}\right) & \sqrt{\kappa_{n,m}^{-1}} \exp\left(j\Phi_{n,m}^{\theta\varphi}\right) \\ \sqrt{\kappa_{n,m}^{-1}} \exp\left(j\Phi_{n,m}^{\varphi\theta}\right) & \exp\left(j\Phi_{n,m}^{\varphi\varphi}\right) \end{bmatrix}$$
$$\begin{bmatrix} F_{tx,s,\theta}\left(\theta_{n,m,ZOD}, \varphi_{n,m,AOD}\right) \\ F_{tx,s,\varphi}\left(\theta_{n,m,ZOD}, \varphi_{n,m,AOD}\right) \end{bmatrix} \exp\left(j2\pi \frac{\hat{r}_{rx,n,m}^T . \overline{d}_{rx,u}}{\lambda_0}\right) \exp\left(j2\pi \frac{\hat{r}_{tx,n,m}^T . \overline{d}_{tx,s}}{\lambda_0}\right) \exp\left(j2\pi \frac{\hat{r}_{rx,n,m}^T . \overline{v}}{\lambda_0} t\right)$$

where $F_{rx,u,\theta}$ and $F_{rx,u,\varphi}$ are the field patterns of receive antenna element *u* in the direction of the spherical basis vectors, $\hat{\theta}$ and $\hat{\varphi}$ respectively, $F_{tx,s,\theta}$ and $F_{tx,s,\varphi}$ are the field patterns of transmit antenna element *s* in the direction of the spherical basis vectors, $\hat{\theta}$ and $\hat{\varphi}$ respectively.

$\hat{r}_{rx,n,m}$ is the spherical unit vector with azimuth arrival angle $\varphi_{n,m,AOA}$ and elevation arrival angle $\theta_{n,m,ZOA}$, given by:

$$\hat{r}_{rx,n,m} = \begin{bmatrix} \sin\theta_{n,m,ZOA}\cos\varphi_{n,m,AOA} \\ \sin\theta_{n,m,ZOA}\sin\varphi_{n,m,AOA} \\ \cos\theta_{n,m,ZOA} \end{bmatrix}$$

where *n* denotes a cluster and *m* denotes a ray within cluster *n*.

$\hat{r}_{tx,n,m}$ is the spherical unit vector with azimuth departure angle $\varphi_{n,m,AOD}$ and elevation departure angle $\theta_{n,m,ZOD}$, given by:

$$\hat{r}_{tx,n,m} = \begin{bmatrix} \sin\theta_{n,m,ZOD}\cos\varphi_{n,m,AOD} \\ \sin\theta_{n,m,ZOD}\sin\varphi_{n,m,AOD} \\ \cos\theta_{n,m,ZOD} \end{bmatrix}$$

where *n* denotes a cluster and *m* denotes a ray within cluster *n*.

$\overline{d}_{rx,u}$ is the location vector of receive antenna element *u* and $\overline{d}_{tx,s}$ is the location vector of transmit antenna element s, $K_{n,m}$ is the cross-polarisation power ratio in linear scale, and λ_0 is the wavelength of the carrier frequency. If polarisation is not considered, the 2×2 polarisation matrix can be replaced by the scalar $exp(j\Phi_{n,m})$ and only vertically polarised field patterns are applied.

The Doppler frequency component depends on the arrival angles (AOA, ZOA), and the UT velocity vector $\overline{\boldsymbol{v}}$ with speed *v*, travel azimuth angle φ_v, elevation angle θ_v and is given by:

$$v_{n,m} = \frac{\hat{r}_{rx,n,m}^{T}\cdot\overline{v}}{\lambda_0}, \text{where } \overline{v} = v.\left[\sin\theta_v\cos\phi_v \quad \sin\theta_v\sin\phi_v \quad \cos\theta_v\right]^T$$

For the two strongest clusters, say n = 1 and 2, rays are spread in delay to three sub-clusters (per cluster), with a fixed delay offset.

The delays of the sub-clusters are

$$\tau_{n,1} = \tau_n$$
$$\tau_{n,2} = \tau_n + 1.28\ c_{DS}$$
$$\tau_{n,3} = \tau_n + 2.56\ c_{DS}$$

where C_{DS} is the cluster delay spread, the values for which are given in the document.

The twenty rays within these two clusters are mapped to three sub clusters as shown below:

Sub-cluster information for intra cluster delay spread clusters

sub-cluster # i	mapping to rays $\mathcal{R}_i$	Power $\lvert\mathcal{R}_i\rvert/M$	delay offset $\tau_{n,i}-\tau_n$
$i=1$	$\mathcal{R}_1=\{1,2,3,4,5,6,7,8,19,20\}$	10/20	0
$i=2$	$\mathcal{R}_2=\{9,10,11,12,17,18\}$	6/20	1.28 c_{DS}
$i=3$	$\mathcal{R}_3=\{13,14,15,16\}$	4/20	2.56 c_{DS}

The channel impulse response is then given by:

$$H_{u,s}^{\mathrm{NLOS}}(\tau,t)=\sum_{n=1}^{2}\sum_{i=1}^{3}\sum_{m\in\mathcal{R}_i}H_{u,s,n,m}^{\mathrm{NLOS}}(t)\delta(\tau-\tau_{n,i})+\sum_{n=3}^{N}H_{u,s,n}^{\mathrm{NLOS}}(t)\delta(\tau-\tau_n)$$

where $H_{u,s,n,m}^{\mathrm{NLOS}}(t)$ is defined as:

$$H_{u,s,n,m}^{\mathrm{NLOS}}(t)=\sqrt{\frac{P_n}{M}}\begin{bmatrix}F_{rx,u,\theta}\left(\theta_{n,m,ZOA},\varphi_{n,m,AOA}\right)\\F_{rx,u,\varphi}\left(\theta_{n,m,ZOA},\varphi_{n,m,AOA}\end{bmatrix}^{T}\begin{bmatrix}\exp\left(j\Phi_{n,m}^{\theta\theta}\right) & \sqrt{\kappa_{n,m}^{-1}}\exp\left(j\Phi_{n,m}^{\theta\varphi}\right)\\\sqrt{\kappa_{n,m}^{-1}}\exp\left(j\Phi_{n,m}^{\varphi\theta}\right) & \exp\left(j\Phi_{n,m}^{\varphi\varphi}\right)\end{bmatrix}$$
$$\begin{bmatrix}F_{tx,s,\theta}\left(\theta_{n,m,ZOD},\varphi_{n,m,AOD}\right)\\F_{tx,s,\varphi}\left(\theta_{n,m,ZOD},\varphi_{n,m,AOD}\right)\end{bmatrix}\exp\left(j2\pi\frac{\hat{r}_{rx,n,m}^{T}\cdot\bar{d}_{rx,u}}{\lambda_0}\right)\exp\left(j2\pi\frac{\hat{r}_{tx,n,m}^{T}\cdot\bar{d}_{tx,s}}{\lambda_0}\right)\exp\left(j2\pi\frac{\hat{r}_{rx,n,m}^{T}\cdot\bar{v}}{\lambda_0}t\right)$$

In the above equations, δ(.) is the Dirac delta function.

The channel response is generated by adding the LOS channel coefficient to the NLOS channel impulse response and scaling the two terms by the desired Ricean K factor K_R.

$$H_{u,s}^{\mathrm{LOS}}(\tau,t)=\sqrt{\frac{1}{K_R+1}}H_{u,s}^{\mathrm{NLOS}}(\tau,t)+\sqrt{\frac{K_R}{K_R+1}}H_{u,s,1}^{\mathrm{LOS}}(t)\delta(\tau-\tau_1)$$

Channel impulse response generation for antenna arrays (Multiple antenna panels at both tx and rx)

Arrangement of the antenna arrays

The antenna panel which is arranged in a uniform rectangular array and the cross-polarised elements within them are arranged as shown below.

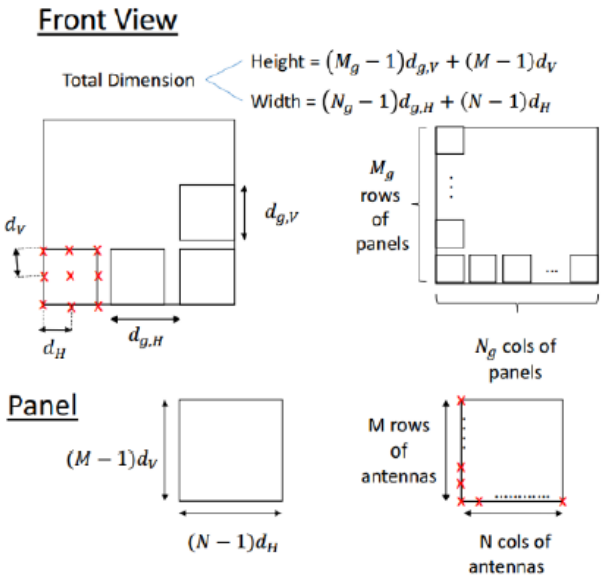

where,

- *Mg* and *Ng* are number of panels in a column and row respectively.
- Antenna panels are uniformly spaced with a center to center spacing of $dg,_H$ and $dg,_V$ in the horizontal and vertical direction respectively.
- Each antenna panel has *M*×*N* antenna elements (single or dual polarized), where *N* is the number of columns and *M* is the number of antenna elements with the same polarization in each column.
- The antenna elements are spaced uniformly with a centre-to-centre distance of d_H horizontally and d_V vertically.

In case of a single cross polarized antenna, *Mg = Ng = M = N =1*. In case of a uniform rectangular array of cross polarized antennas with no sub arrays *Mg = Ng = 1.*

Vector channel response

Using antenna arrays at the transmitter and receiver results in a vector channel response. The LOS channel coefficient and NLOS channel impulse response for each cluster *n* is given below:

$$\mathbf{H}_n^{\mathrm{NLOS}}(t)=\sqrt{\frac{P_n}{M}}\sum_{m=1}^{M}\begin{bmatrix}F_{\mathrm{rx},\theta}\left(\theta_{n,m,ZOA},\phi_{n,m,AOA}\right)\\F_{\mathrm{rx},\phi}\left(\theta_{n,m,ZOA},\phi_{n,m,AOA}\right)\end{bmatrix}^{T}\begin{bmatrix}\exp\left(j\Phi_{n,m}^{\theta\theta}\right) & \sqrt{\kappa_{n,m}^{-1}}\exp\left(j\Phi_{n,m}^{\theta\phi}\right)\\\sqrt{\kappa_{n,m}^{-1}}\exp\left(j\Phi_{n,m}^{\phi\theta}\right) & \exp\left(j\Phi_{n,m}^{\phi\phi}\right)\end{bmatrix}$$
$$\times\begin{bmatrix}F_{\mathrm{tx},\theta}\left(\theta_{n,m,ZOD},\phi_{n,m,AOD}\right)\\F_{\mathrm{tx},\phi}\left(\theta_{n,m,ZOD},\phi_{n,m,AOD}\right)\end{bmatrix}\mathbf{a}_{\mathrm{rx}}\left(\theta_{n,m,ZOA},\phi_{n,m,AOA}\right)\mathbf{a}_{\mathrm{tx}}^{\mathrm{H}}\left(\theta_{n,m,ZOD},\phi_{n,m,AOD}\right)\exp\left(j2\pi\nu_{n,m}t\right)$$

$$\mathbf{H}_n^{\mathrm{LOS}}(t)=\begin{bmatrix}F_{\mathrm{rx},\theta}\left(\theta_{LOS,ZOA},\phi_{LOS,AOA}\right)\\F_{\mathrm{rx},\phi}\left(\theta_{LOS,ZOA},\phi_{LOS,AOA}\right)\end{bmatrix}^{T}\begin{bmatrix}\exp\left(j\Phi_{LOS}\right) & 0\\0 & \exp\left(j\Phi_{LOS}\right)\end{bmatrix}$$
$$\times\begin{bmatrix}F_{\mathrm{tx},\theta}\left(\theta_{LOS,ZOD},\phi_{LOS,AOD}\right)\\F_{\mathrm{tx},\phi}\left(\theta_{LOS,ZOD},\phi_{LOS,AOD}\right)\end{bmatrix}\mathbf{a}_{\mathrm{rx}}\left(\theta_{LOS,ZOA},\phi_{LOS,AOA}\right)\mathbf{a}_{\mathrm{tx}}^{\mathrm{H}}\left(\theta_{LOS,ZOD},\phi_{LOS,AOD}\right)\exp\left(j2\pi\nu_{\mathrm{LOS}}t\right)$$

where $\mathbf{a}_{rx}(\theta_{n,m,ZOA}, \varphi_{n,m,AOA})$ and $\mathbf{a}_{tx}(\theta_{n,m,ZOD}, \varphi_{n,m,AOD})$ are the rx and tx antenna array response vectors respectively, of rays $m \in 1, 2, M$ in the cluster $n \in 1, 2, \ldots, N$. They are given by:

$$\mathbf{a}_{\mathrm{tx}}\left(\theta_{n,m,ZOD},\phi_{n,m,AOD}\right)=\exp(j\frac{2\pi}{\lambda}(\mathbf{W}_{tx}\mathbf{r}_{\mathrm{tx}}(\theta_{n,m,ZOD},\phi_{n,m,AOD}))),\forall n,m,$$

$$\mathbf{a}_{\mathrm{rx}}\left(\theta_{n,m,ZOA},\phi_{n,m,AOA}\right)=\exp(j\frac{2\pi}{\lambda}(\mathbf{W}_{\mathrm{rx}}\mathbf{r}_{\mathrm{rx}}(\theta_{n,m,ZOA},\phi_{n,m,AOA}))),\forall n,m,$$

where λ is the wavelength of the carrier frequency f, $\mathbf{r}_{rx}(\theta_{n,m,ZOA}, \varphi_{n,m,AOA})$ and $\mathbf{r}_{tx}(\theta_{n,m,ZOD}, \varphi_{n,m,AOD})$ are the corresponding angular 3 x 1 spherical unit vectors of the rx and tx, respectively.

$\mathbf{W}_{tx}$ and $\mathbf{W}_{rx}$ are the location matrices of the tx and rx antenna elements in 3D Cartesian coordinates, which are provided for a uniform rectangular array antenna configuration consisting of cross polarized antenna elements and for the arrangement discussed above earlier. For the uniform rectangular array configuration discussed above, $\mathbf{W}_{tx}$ and $\mathbf{W}_{rx}$ are matrices of the dimension $2NMN_gM_g$ x 3.

$\mathbf{W}_{tx}$ for example, = [w_{ij}] i=1, 2..., $2NMN_gM_g$, j =1,2,3, where

$$w_{ij}=\begin{cases}0, & j=1\\\left\lfloor\left(i-1-2N\left\lfloor\frac{i-1}{2N}\right\rfloor\right)\Big/2\right\rfloor\cdot d_H+\left\lfloor\left(i-1-2NN_g\left\lfloor\frac{i-1}{2NN_g}\right\rfloor\right)\Big/(2N)\right\rfloor\cdot d_{g,H}, & j=2\\\left\lfloor\left(i-1-2NMN_g\left\lfloor\frac{i-1}{2NMN_g}\right\rfloor\right)\Big/(2NN_g)\right\rfloor\cdot d_V+\left\lfloor\left(i-1-2NMN_gM_g\left\lfloor\frac{i-1}{2NMN_gM_g}\right\rfloor\right)\Big/(2NMN_g)\right\rfloor\cdot d_{g,V}, & j=3\end{cases}$$

3.3 Field pattern generation: ([5])

The field patterns, $F_{tx,\theta}(\theta, \phi)$, $F_{tx,\varphi}(\theta, \phi)$, $F_{rx,\theta}(\theta, \phi)$ and $F_{rx,\varphi}(\theta, \phi)$ are generated by converting GCS into LCS coordinate system.

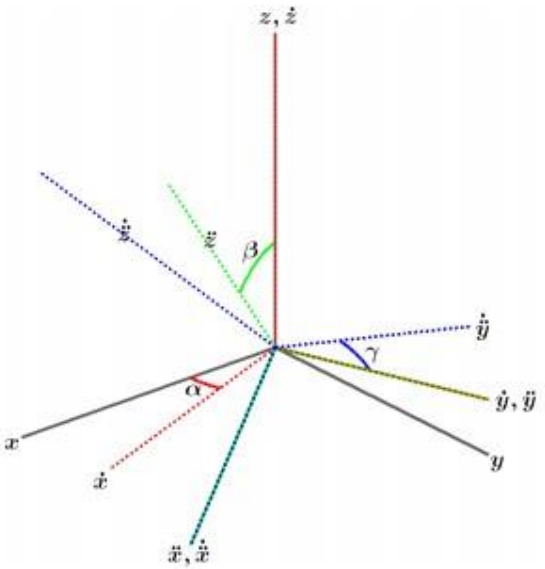

Figure 7.1.3-1: Orienting the LCS (blue) with respect to the GCS (gray) by a sequence of 3 rotations: α, β, γ.

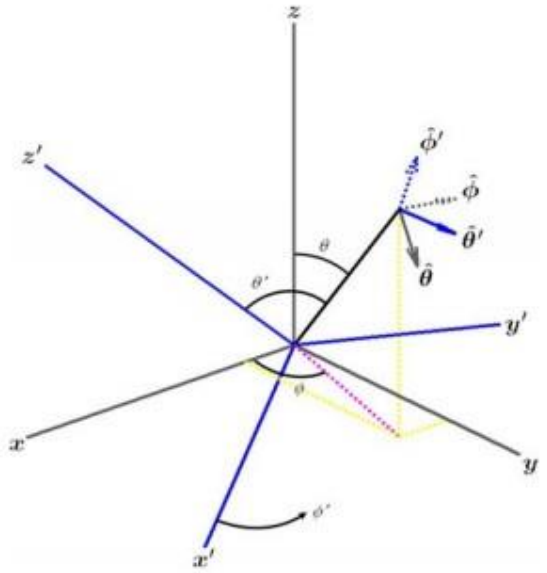

Figure 7.1.3-2: Definition of spherical coordinates and unit vectors in both the GCS and LCS.

Figure 3.7

The filed patterns are given by,

$$\begin{pmatrix} F_\theta(\theta,\phi) \\ F_\phi(\theta,\phi) \end{pmatrix} = \begin{pmatrix} +\cos\psi & -\sin\psi \\ +\sin\psi & +\cos\psi \end{pmatrix} \begin{pmatrix} F'_{\theta'}(\theta',\phi') \\ F'_{\phi'}(\theta',\phi') \end{pmatrix}$$

Where,

$$\theta'(\alpha,\beta,\gamma;\theta,\phi) = \arccos\left(\begin{bmatrix} 0 \\ 0 \\ 1 \end{bmatrix}^T R^{-1}\hat{\rho} \right) = \operatorname{acos}(\cos\beta\cos\gamma\cos\theta + (\sin\beta\cos\gamma\cos(\phi-\alpha) - \sin\gamma\sin(\phi-\alpha))\sin\theta)$$

$$\phi'(\alpha,\beta,\gamma;\theta,\phi) = \arg\left(\begin{bmatrix} 1 \\ j \\ 0 \end{bmatrix}^T R^{-1}\hat{\rho} \right) = \arg\begin{pmatrix} (\cos\beta\sin\theta\cos(\phi-\alpha) - \sin\beta\cos\theta) + \\ j(\cos\beta\sin\gamma\cos\theta + (\sin\beta\sin\gamma\cos(\phi-\alpha) + \cos\gamma\sin(\phi-\alpha))\sin\theta) \end{pmatrix}$$

$$\psi = \arg\begin{pmatrix}(\sin\gamma\cos\theta\sin(\phi-\alpha)+\cos\gamma(\cos\beta\sin\theta-\sin\beta\cos\theta\cos(\phi-\alpha)))+\\ j(\sin\gamma\cos(\phi-\alpha)+\sin\beta\cos\gamma\sin(\phi-\alpha))\end{pmatrix}$$

And the F prime values are given by,

$$\begin{pmatrix}F'_{\theta'}(\theta',\phi')\\ F'_{\phi'}(\theta',\phi')\end{pmatrix}=\begin{pmatrix}+\cos\psi & -\sin\psi\\ +\sin\psi & +\cos\psi\end{pmatrix}\begin{pmatrix}F''_{\theta''}(\theta'',\phi'')\\ F''_{\phi''}(\theta'',\phi'')\end{pmatrix}$$

Where,

$$\theta'' = \theta' \text{ and } \phi'' = \phi'$$

$$\cos\psi=\frac{\cos\zeta\sin\theta'+\sin\zeta\sin\phi'\cos\theta'}{\sqrt{1-(\cos\zeta\cos\theta'-\sin\zeta\sin\phi'\sin\theta')^2}},\ \sin\psi=\frac{\sin\zeta\cos\phi'}{\sqrt{1-(\cos\zeta\cos\theta'-\sin\zeta\sin\phi'\sin\theta')^2}}$$

ζ= +/- 45 degrees corresponding to a pair of cross-polarized antenna elements or 0 degrees corresponds to a purely vertically polarized antenna element.

For a single polarized antenna (purely vertically polarized antenna) we can write

$F''_{\theta}\left(\theta'',\phi''\right)=\sqrt{A''\left(\theta'',\phi''\right)}$ and $F''_{\phi}\left(\theta'',\phi''\right)=0$

And for cross-polarized antenna elements, the field pattern in both directions are equally distributed.

$$A''(\theta'',\phi'')=\left|F''_{\theta''}(\theta'',\phi'')\right|^2+\left|F''_{\phi''}(\theta'',\phi'')\right|^2$$

The Antenna radiation patterns for both BS and UT are given in the ITU-R M.2412 document.

Step 12: Path loss and shadowing

The path loss models and their applicability, including frequency ranges and the LOS probability, for the 4 cases of test environments are given in ITU-R M.2412.

Shadow fading is modelled as log-normal and the corresponding standard deviation are mentioned along as well. Apply path loss and shadowing for the channel coefficients.

CHAPTER 4 - Results and Discussion

4.1 ANTENNA RADIATION PATTERN (contributed by my project mate M.S. Ajay)

We generated Radiation pattern of single antenna element using our code and the pattern is shown in the following images (see fig – 4.1, 4.2, 4.3)

These are generated keeping bearing angle (α), down tilt angle (β) and slant angle (γ) at "**0 degrees"**.

Depending upon those angles, the directivity of max gain (here ***8dBi***) keeps changing.

Changing **α** rotates directivity along **z axis**, **β** along **y axis** and **γ** along **x axis** respectively.

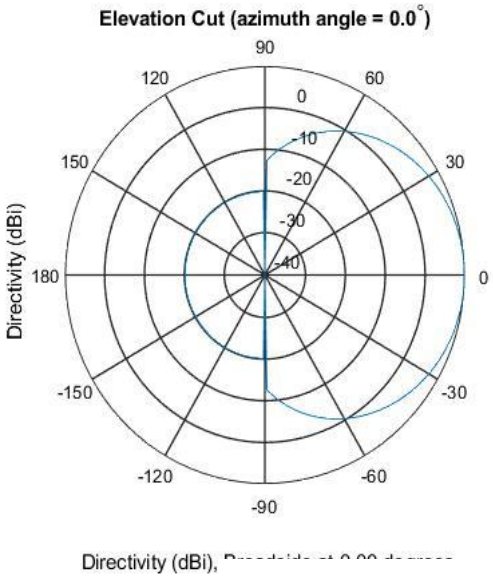

Figure 4.1

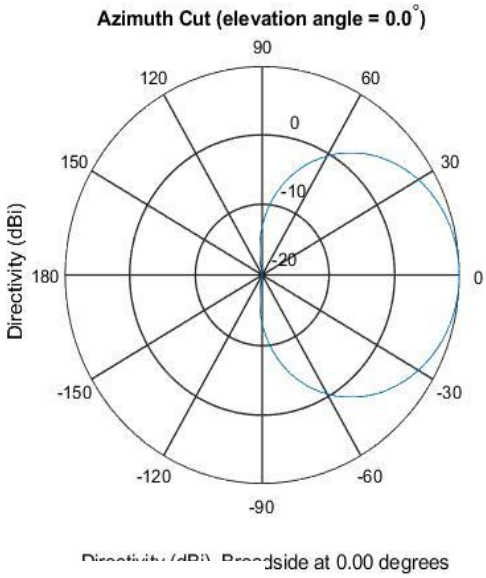

Figure 4.2

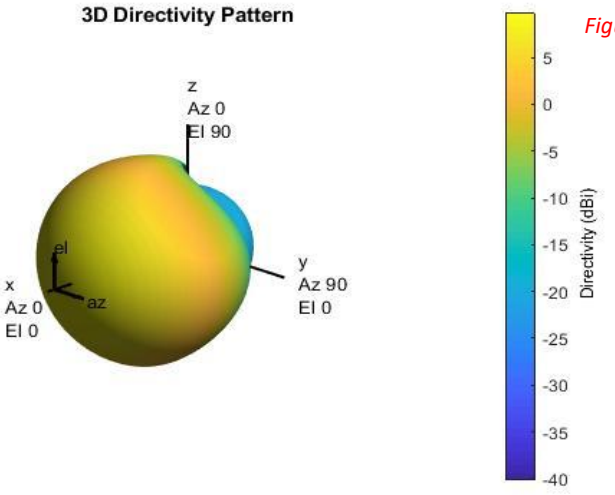

Figure 4.3

We also generated the radiation pattern for an antenna array (see figures – 4.4, 4.5, 4.6). This is for an array of "***6x6".*** We can observe the antenna power increased from ***8dBi*** to ***20dBi.*** This is another reason we use antenna arrays in transmitting.

We can also see how it is varying along azimuthal direction in fig- 4.5 and how it is varying along elevational direction in fig - 4.4

NOTE: All the generated radiation patterns are from BASESTATION Antennas.

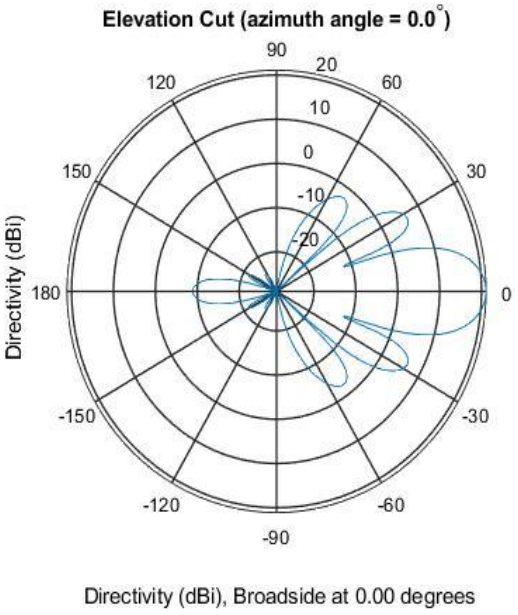

Figure 4.4

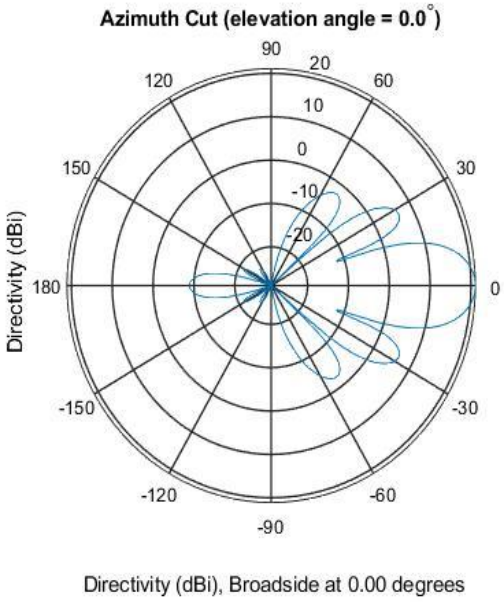

Figure 4.5

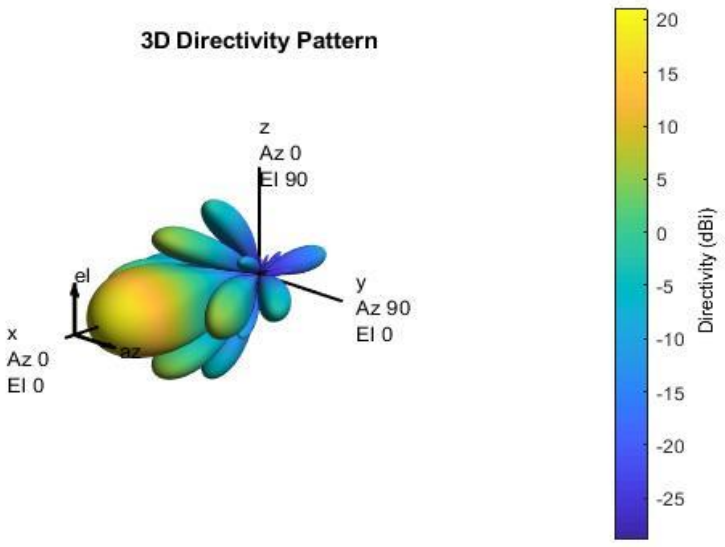

Figure 4.6

4.2 CHANNEL ESTIMATION (contributed by me)

After generating the channel coefficients, we interpolate them using **SINC** function to get the coefficients at regular intervals of **1/BW,** from (0 to T/BW) and we calculate required no. of taps at each time interval.

We use this final H_COEFF matrix for the convolution of input signal to get the output signal. (Refer SCM_TEST_VESCTORS file in the code).

From this output signal we estimate our channel H. Some of the simulation results are shown below (in figures- 4.7, 4.8, 4.9, 4.10).

There are 3072 sub-carriers and the plot shows the channel gain at each sub-carrier.

RMa_A:

Center frequency = 700 MHz, Bandwidth = 122.88 MHz, in car = 'FALSE' and indoor = 'OUTDOOR'

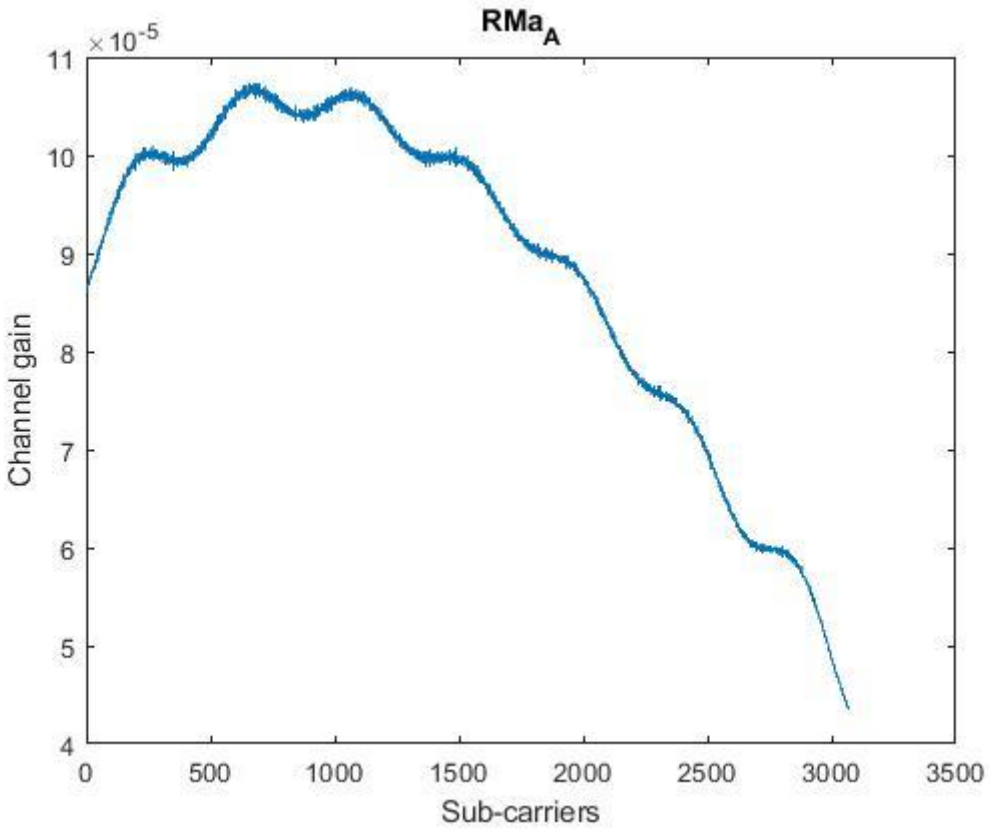

Figure 4.7

UMa_A:

Center frequency = 4GHz, Bandwidth = 122.88 MHz, in car = 'FALSE' and indoor = 'OUTDOOR'.

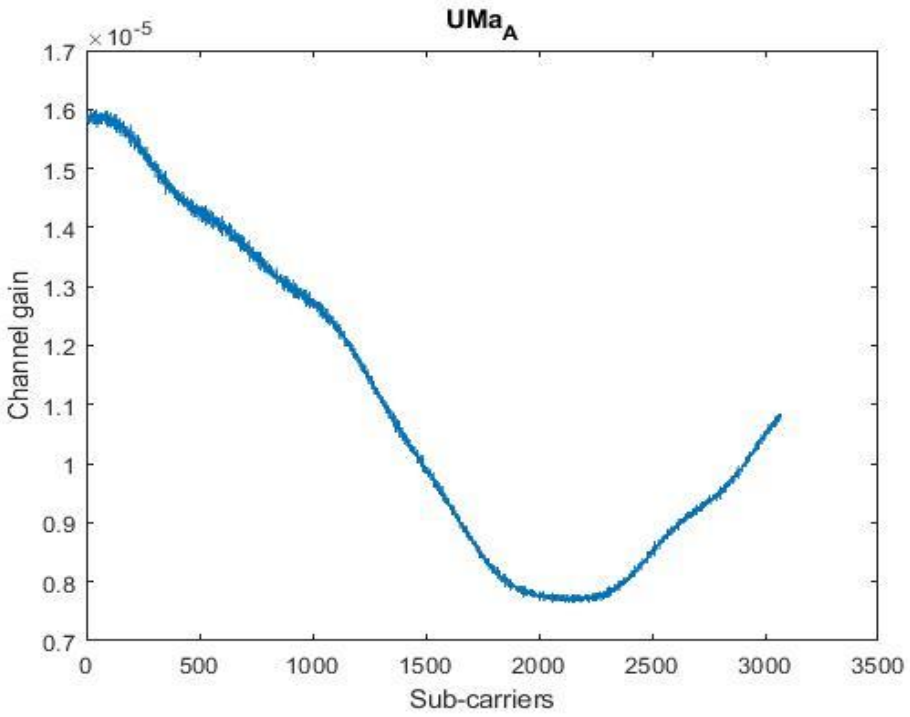

Figure 4.8

UMi_A:

Center frequency = 4GHz, Bandwidth = 122.88 MHz, in car = 'FALSE' and indoor = 'OUTDOOR'.

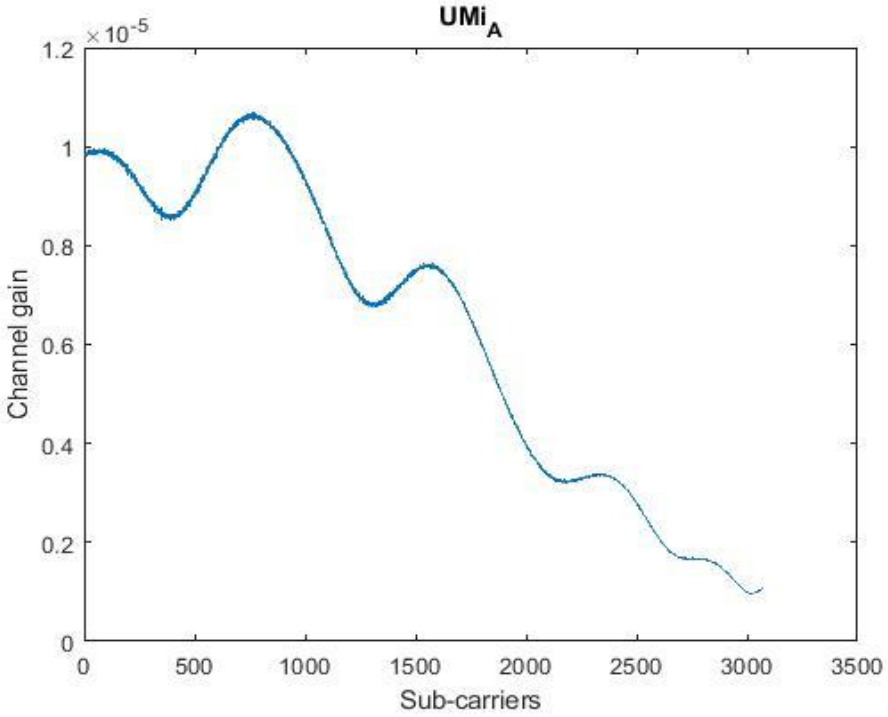

Figure 4.9

InH_A:

Center frequency = 4GHz, Bandwidth = 122.88 MHz, in car = 'FALSE' and indoor = 'OUTDOOR'.

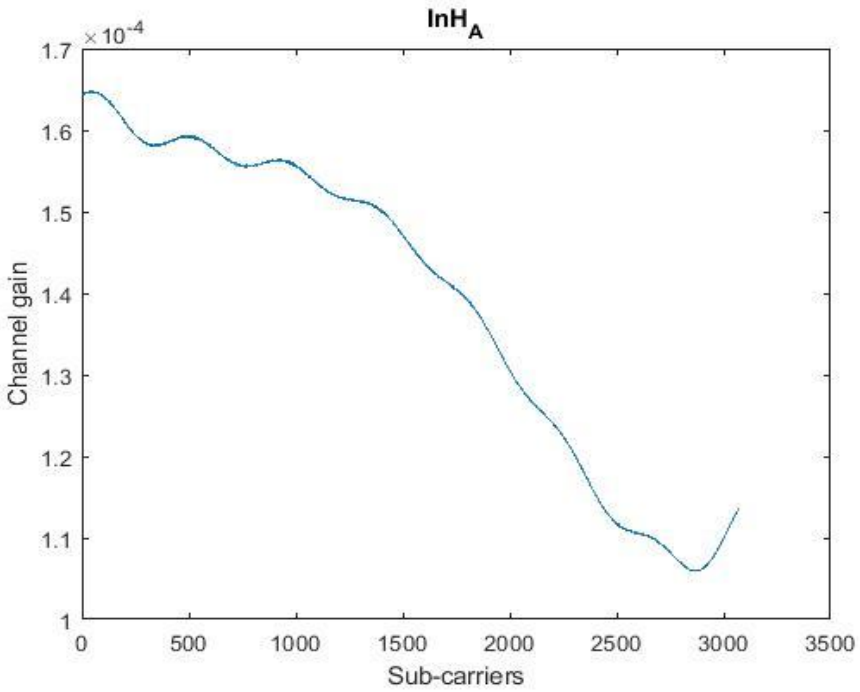

Figure 4.10

4.3 SINR GENERATION (contributed by M.S. AJAY)

We also generated SINR, using the Antenna transmit power from Base stations, directivity radiation power and pathloss.

SINR = transmit power + directivity antenna power – pathloss (in dB).

We generated hexagon grids, placed Base stations in the grid and generated how the SINR looks.

The first figure (fig. 4.11) captures SINR for RURAL profile assuming all the points as LOS and the second figure (fig. 4.12) captures the same assuming all the points as NLOS.

The third (fig. 4.13) and fourth figures ((fig. 4.14) captures the same for URBAN macro for both LOS and NLOS cases.

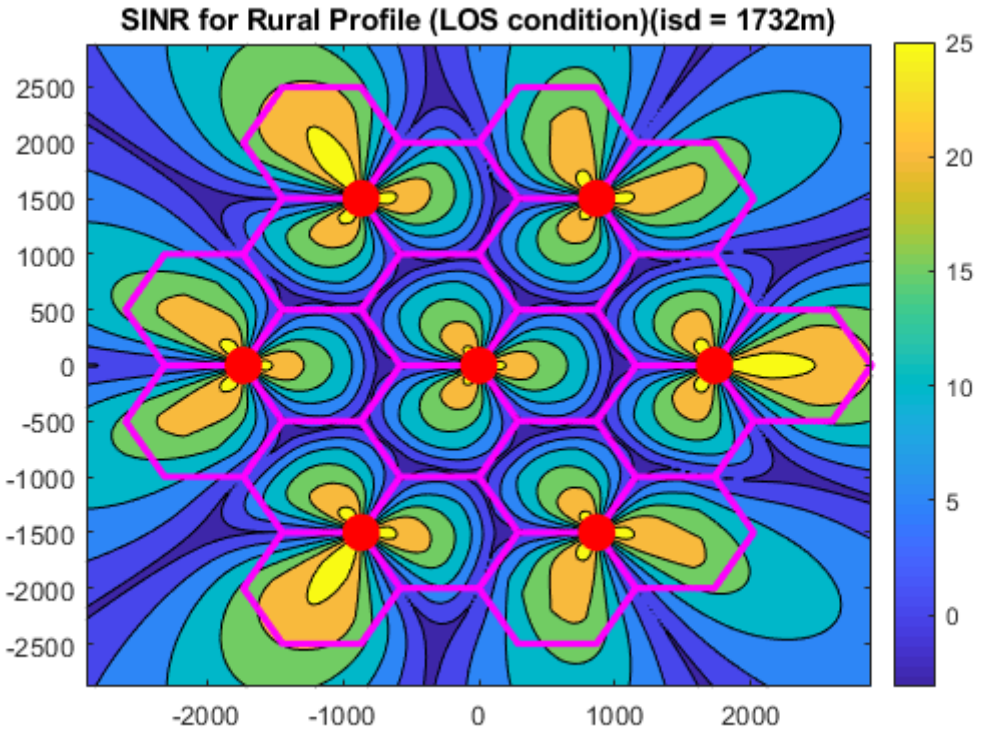

Figure 4.11

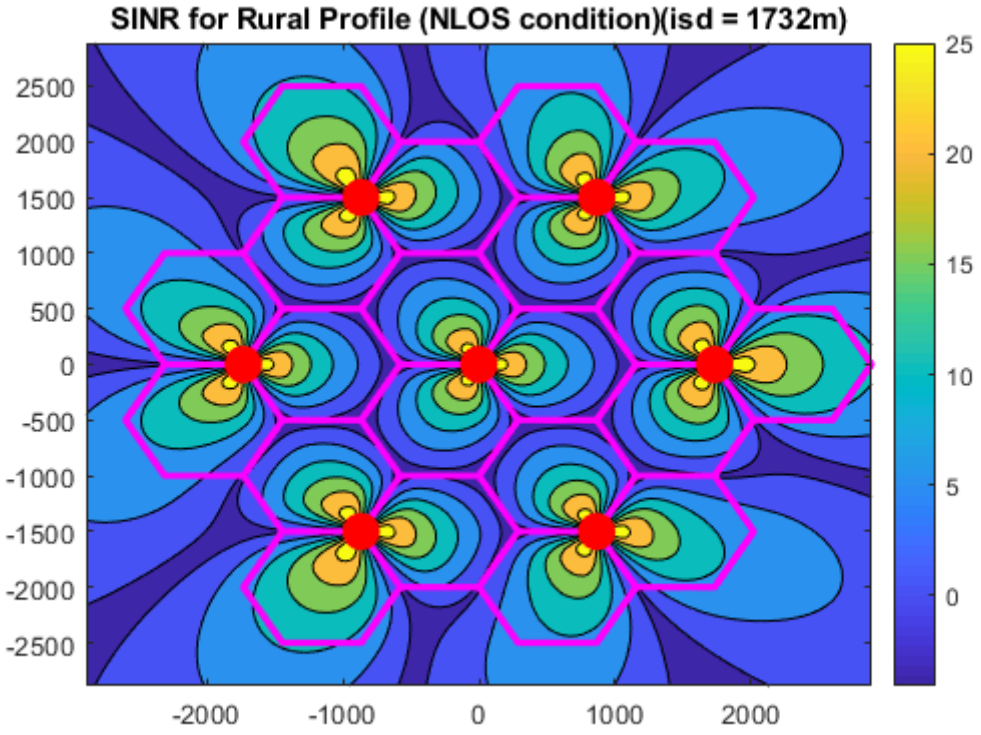

Figure 4.12

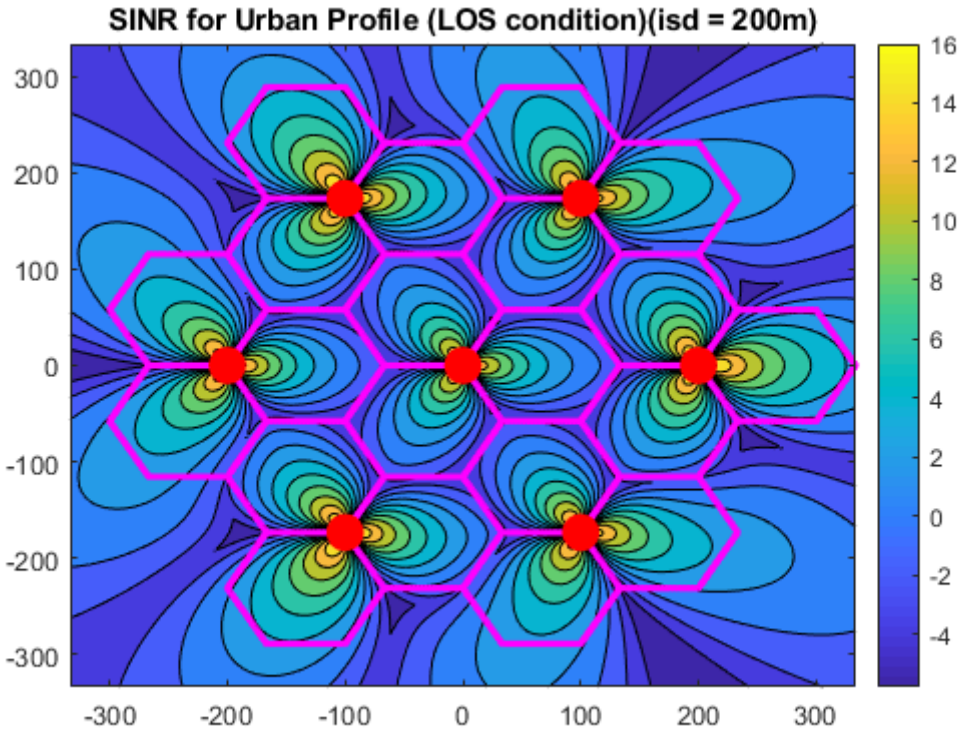

Figure 4.13

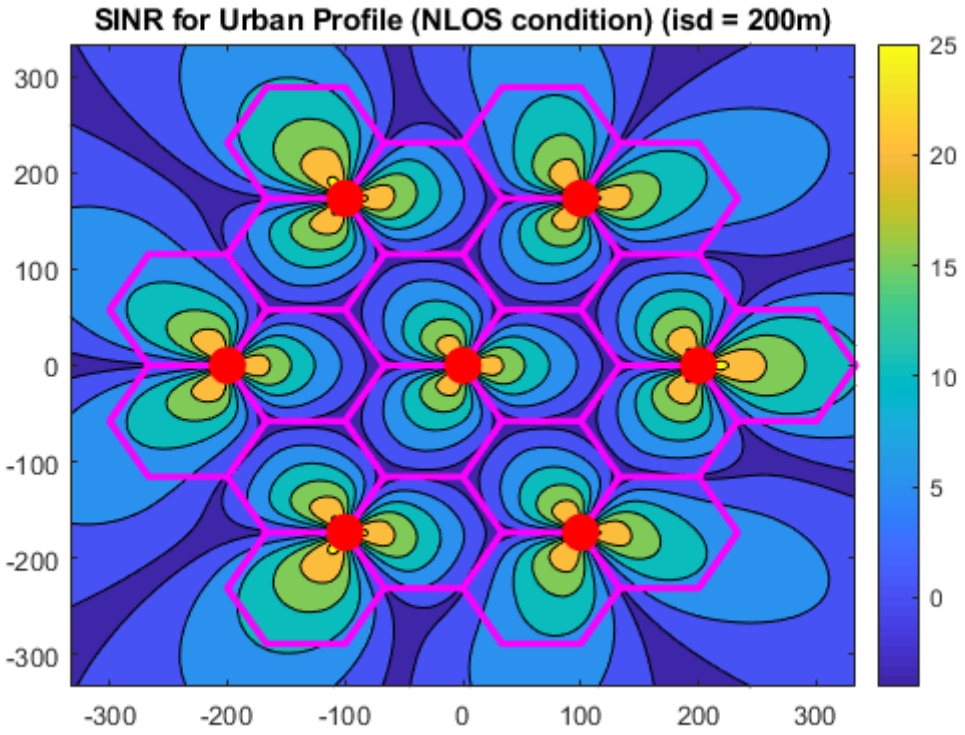

Figure 4.14

CHAPTER 5

Potential extensions and future work

The MATLAB code written is for the case of a single user in a sector. The code has to be extended to be able to support the simulation of multiple gNBs and UEs per sector. Once the codes for a single UE and a single channel link is verified, this extension needs to done and has to be verified in a similar manner, before using them for simulating the test environments for evaluation procedures and measuring the KPIs.

Also the channel model can be further improved for simulating certain test scenarios by incorporating advanced modelling components like Oxygen absorption, random cluster number, ground reflection, UT rotation, blockage, spatial consistency and modelling of propagation delay and intra cluster angular and delay spreads for incorporating large antenna size and large number of antenna elements.

The modelling procedure for the above-mentioned advanced components along with the corresponding step in the channel generation procedure, in which it is to be incorporated and the recommended conditions in which they can be done in addition to the normal channel generation procedure are described in the ITU document M.2412.

Summary

The channel model gives full access to all the configuration parameters. The main advantage of the 3GPP geometry based stochastic channel modelling is that the scatterers are defined based on the angles of departure and angles of arrival, i.e. terminal perspective, rather than defining the physical position of the scatterers in the simulation area like a few other channel models. If physical positions are used, it is difficult to extract parameters using measurements contrary to the case of the GSCM channel model. Hence GSCM is currently more widespread and is the preferred candidate for 5G channel modelling in standardization efforts.

The channel code written is not fully spatially consistent, that is it fails to capture scenarios where the users are in close proximity, as the channels are generated independently for each user, regardless of the distance between users. This can be improved by incorporating the spatial consistency procedure. (Refer ITU-R M.2412-0)

References:

[1] **Report ITU-R M.2410-0**
Minimum requirements related to technical performance for IMT-2020 radio interface(s)

[2] **Report ITU-R M.2411-0**
Requirements, evaluation criteria and submission templates for the development of IMT-2020

[3] **Report ITU-R M.2412-0**
Guidelines for evaluation of radio interface technologies for IMT-2020

[4] **IST-WINNER II Deliverable 1.1.2 v.1.2.,** "WINNER II channel models, IST-WINNER2, Tech. Rep., 2008.

[5] **ETSI TR 138 901 V14.3.0 (2018-01), 3GPP TR 38.901 version 14.3.0 Release 14,** "*5G; Study on channel model for frequencies from 0.5 to 100 GHz*"**.**